

# Vector Precoding for Wireless MIMO Systems and its Replica Analysis

Ralf R. Müller, *Senior Member, IEEE*, Dongning Guo, *Member, IEEE*, and Aris L. Moustakas, *Senior Member, IEEE*

**Abstract**—This paper studies a nonlinear vector precoding scheme which inverts the wireless multiple-input multiple-output (MIMO) channel at the transmitter so that simple symbol-by-symbol detection can be used in lieu of sophisticated multiuser detection at the receiver. In particular, the transmit energy is minimized by relaxing the transmitted symbols to a larger alphabet for precoding, which preserves the minimum signaling distance. The so-called replica method is used to analyze the average energy savings with random MIMO channels in the large-system limit. It is found that significant gains can be achieved with complex-valued alphabets. The analysis applies to a very general class of MIMO channels, where the statistics of the channel matrix enter the result via the R-transform of the asymptotic empirical distribution of its eigenvalues. Moreover, we introduce polynomial-complexity precoding schemes for binary and quadrature phase-shift keying in complex channels by using convex rather than discrete relaxed alphabets. In case the number of transmit antennas is more than twice the number of receive antennas, we show that a convex precoding scheme, despite its polynomial complexity, outperforms NP-hard precoding using the popular Tomlinson-Harashima signaling.

**Index Terms**—Multiple antennas, multiple-input multiple-output (MIMO) systems, spatial equalization, Tomlinson-Harashima precoding, replica method, random matrices, R-transform.

## I. INTRODUCTION

SINCE the pioneer work of [1] and [2], it has been well-known that using multiple transmit and receive antennas with sophisticated signal processing can improve the data rate of wireless systems significantly without need for additional radio spectrum. As a design choice, signal processing can be carried out at the receiver side, the transmitter side, or both. This work studies nonlinear precoding schemes where major processing is required solely at the transmitter, so that signal

detection at the receiver can be simply performed symbol-by-symbol in lieu of joint (or multiuser) detection. Such schemes are obviously advantageous for downlink data transmission to low-cost or battery-driven devices such as cell-phones and wireless sensors.

Assuming that the multiple-input multiple-output (MIMO) channel coefficients are known to the transmitter, the channel can be inverted using a linear precoder so that no crosstalk is seen by the receiver [3], [4]. The convenience comes, however, at the expense of enhancing the transmit energy required to maintain the same received signal-to-noise ratio (SNR). It has been recognized that for transmission with a discrete constellation, the data vector can be perturbed to take values in a relaxed alphabet (usually a subsuming lattice) before linear precoding. This reduces the transmit energy, and yet maintains the minimum distance of the signal constellation [5]–[7]. The technique of nonlinear precoding can be traced back to the work of Tomlinson [8] and Harashima and Miyakawa [9] on inter-symbol interference channels.

The search for a displacement vector corresponding to the minimum-energy signal in a discrete set is an NP-hard problem in general. An exhaustive search is computationally complex and becomes infeasible for large alphabets and/or high dimensions. As a major contribution in this paper, we propose to use non-discrete alphabets, and in particular disjoint convex sets as the relaxed alphabets. If each symbol can be represented by any letter in its corresponding convex set, the search for the minimum energy signal becomes a convex optimization problem, which admits efficient algorithms [10]. Several convex sets of relaxed alphabets are described in the paper which preserve the minimum distance of signaling.

With precoding technique broadened to the use of arbitrary alphabets, whether discrete or not, this paper further studies the energy savings due to nonlinear precoding. Under several assumptions, we use the so-called replica method to quantify the average minimum transmit energy required for maintaining the minimum distance of the signaling in random high-dimensional MIMO systems. To the best of our knowledge, this work puts forth the first analytical formulas for evaluating the minimum transmit energy in nonlinear precoding.

Admittedly, this paper only takes a first step towards a complete characterization of nonlinear precoding, as it should be cautioned that the replica analysis is based on several heuristic assumptions which have not been rigorously justified in mathematical physics. The replica method was originally invented for the analysis of spin glasses in statistical physics

Manuscript received May 30, 2007; revised October 22, 2007. This material is based upon work supported by the Research Council of Norway, the National Science Foundation, DARPA, and the European Commission under Grant Nos. 171133/V30, CCF-0644344, W911NF-07-1-0028, and MIRG-CT-2005-030833 respectively. This paper was presented in part at the 2007 IEEE International Symposium on Information Theory in Nice, France, the 2007 International Workshop on Statistical-Mechanical Informatics in Kyoto, Japan and the 2008 Information Theory and Applications Workshop, San Diego, CA, USA.

R. Müller is with the Department of Electronics and Telecommunications, The Norwegian University of Science and Technology, Trondheim, Norway (e-mail: ralf@iet.ntnu.no).

D. Guo is with the Department of Electrical Engineering and Computer Science, Northwestern University, Evanston, IL, USA (e-mail: dGuo@northwestern.edu).

A. Moustakas is with the Physics Department, National and Kapodistrian University of Athens, Athens, Greece (e-mail: arislm@phys.uoa.gr).

Digital Object Identifier 10.1109/JSAC.2008.080411.

[11], [12] and has recently been successfully applied to problems in wireless communications (e.g. [13]–[16]) and coding theory (e.g. [17], [18]). Extensive simulation and exact analytical results in the literature suggest that the replica analysis generally yields excellent approximations in random MIMO systems.

The paper is composed of five more sections. Section II introduces vector precoding with arbitrary alphabets. Section III presents the general result for the minimum transmit energy in high-dimensional channels. Section IV specializes the results to MIMO channels and various choices of relaxed alphabets. Conclusions are drawn in Section V. Some technical details including the replica analysis are relegated to the Appendix.

## II. VECTOR PRECODING

Consider a single-user MIMO system described by

$$\mathbf{r} = \mathbf{H}\mathbf{t} + \mathbf{n} \quad (1)$$

where the vectors  $\mathbf{t}$  and  $\mathbf{r}$  denote the signals at the multiple transmit and received antennas respectively,  $\mathbf{H}$  denotes the  $K \times N$  matrix of antenna gains, and  $\mathbf{n}$  denotes the white Gaussian noise. Instead of directly modulating the data stream onto the  $N$  transmit antennas, vector precoding maps the  $K$ -dimensional vector of data symbols  $\mathbf{s}$  to the  $N$ -dimensional signal  $\mathbf{t} = T(\mathbf{s})$  for transmission.

This paper studies the following nonlinear precoding scheme which aims to simplify the receiver as well as to minimize the transmit energy. Let us assume not more receive antennas than transmit antennas for now ( $K \leq N$ ). Consider first linear precoding with the pseudoinverse of the channel

$$\mathbf{T} = \mathbf{H}^+ = \mathbf{H}^\dagger (\mathbf{H}\mathbf{H}^\dagger)^{-1} \quad (2)$$

so that the received signal becomes

$$\mathbf{r} = \mathbf{H}\mathbf{T}\mathbf{x} + \mathbf{n} = \mathbf{x} + \mathbf{n} \quad (3)$$

where the signal  $\mathbf{x}$  represents the same data as  $\mathbf{s}$  does. Evidently, the symbols observed at the received antennas are completely separated and can be simply detected symbol-by-symbol. Instead of letting  $\mathbf{x} = \mathbf{s}$ , which reduces to linear precoding, we choose the entries of  $\mathbf{x}$  from a relaxed alphabet which induces a smaller transmit energy.

Specifically, let  $\mathcal{S}$  denote the original signal constellation, i.e.,  $\mathbf{s} = [s_1, \dots, s_K] \in \mathcal{S}^K$ . The relaxed alphabet (constellation)  $\mathcal{B}$  is then a union of some disjoint sets  $\mathcal{B}_s$ ,  $s \in \mathcal{S}$ , so that every symbol  $s \in \mathcal{S}$  can be represented using any element in  $\mathcal{B}_s$  without ambiguity. In particular, the vector  $\mathbf{s}$  is mapped to some vector  $\mathbf{x} = [x_1, \dots, x_K]^\top$  with  $x_k \in \mathcal{B}_{s_k}$ ,  $k = 1, \dots, K$ , which minimizes the transmit energy, i.e.,

$$\mathbf{x}^* = \underset{\mathbf{x} \in \mathcal{B}_{s_1} \times \dots \times \mathcal{B}_{s_K}}{\operatorname{argmin}} \|\mathbf{T}\mathbf{x}\|^2. \quad (4)$$

One would also like to design the subsets  $\mathcal{B}_s$  to satisfy the following distance-preserving property

$$\|s - s'\| \leq \min_{x \in \mathcal{B}_s, x' \in \mathcal{B}_{s'}} \|x - x'\|, \quad \forall s, s' \in \mathcal{S} \quad (5)$$

i.e., the minimum distance between the represented data symbols does not decrease due to the mapping. This is easily achieved by letting  $\mathcal{B}_s$  be distinct sub-lattices of  $\mathcal{B}$  with  $s \in \mathcal{B}_s$

for every  $s \in \mathcal{S}$ . Strictly speaking, using a relaxed alphabet may increase the uncoded error probability even though the minimum distance is preserved. Such an impact is negligible at moderate to high SNRs.

Note that in case of more receive antennas than transmit antennas ( $K > N$ ), the channel cannot be inverted using any linear precoder. We still define the precoding matrix as the (Moore-Penrose) pseudoinverse [19]

$$\mathbf{T} = \mathbf{H}^+ = \lim_{\epsilon \rightarrow 0} \mathbf{H}^\dagger (\mathbf{H}\mathbf{H}^\dagger + \epsilon \mathbf{I})^{-1} \quad (6)$$

where the limit exists although  $\mathbf{H}\mathbf{H}^\dagger$  is not invertible, but we modify the objective function of the constrained optimization (4) to read

$$\mathbf{x}^* = \underset{\mathbf{x} \in \mathcal{B}_{s_1} \times \dots \times \mathcal{B}_{s_K}}{\operatorname{argmin}} \lim_{\epsilon \rightarrow 0} \mathbf{x}^\dagger (\mathbf{H}\mathbf{H}^\dagger + \epsilon \mathbf{I})^{-1} \mathbf{x}. \quad (7)$$

Note that if  $\mathbf{T}\mathbf{s}$  is transmitted, there will be crosstalk in the received vector because  $\mathbf{H}\mathbf{H}^+ \neq \mathbf{I}$ . Remarkably, if we transmit  $\mathbf{T}\mathbf{x}$  with the minimum energy representing the same data, then there is typically no crosstalk as long as  $K$  is not greater than a threshold  $K^* > N$ , because the relaxed vector  $\mathbf{x}$  can usually be found in the subspace spanned by those columns of  $\mathbf{H}$  which can effectively be inverted by  $\mathbf{H}^+$ .

We finish the description of vector precoding using an example of relaxed alphabets for binary transmission. Without precoding, it is most common to map each bit to one of the two symbols in  $\mathcal{S} = \{-1, +1\}$ , which is known as binary phase shift keying (BPSK). With vector precoding, a popular choice for the supersets is  $\mathcal{B}_{-1} = 4\mathbb{Z} - 1$  and  $\mathcal{B}_{+1} = 4\mathbb{Z} + 1$  [8], [9], which is known as the Tomlinson-Harashima precoding. The distance property (5) obviously holds.

## III. GENERAL RESULTS

Given the precoding matrix  $\mathbf{T}$  and the disjoint alphabets  $\mathcal{B}_s$ ,  $s \in \mathcal{S}$ , solving (4) for the minimum energy signal is known as a quadratic programming problem in the optimization literature, which is computationally complex in general. For example, the problem is NP-hard with the discrete lattice alphabets in the Tomlinson-Harashima precoding.

In this work, we broaden the scope of vector precoding to include the use of arbitrary alphabets which may or may not be discrete, as long as the distance-preserving property (5) holds. In particular, we propose several sets of convex alphabets, which reduce (4) and (7) to convex optimization problems because the respective objective functions are strictly positive. Efficient algorithms with polynomial complexity can then be applied. We relegate the discussion of various precoding alphabets and their performance to Section IV. In the following, we focus on the result of the minimum transmit energy with an arbitrary set of given alphabets, either convex or not.

Formally, the expected transmit energy per dimension of the precoding scheme described in Section II is

$$\frac{1}{K} \mathbb{E} \left\{ \min_{\mathbf{x} \in \mathcal{B}_{s_1} \times \dots \times \mathcal{B}_{s_K}} \lim_{\epsilon \rightarrow 0} \mathbf{x}^\dagger (\mathbf{H}\mathbf{H}^\dagger + \epsilon \mathbf{I})^{-1} \mathbf{x} \right\} \quad (8)$$

where the expectation is over the distribution of the channel matrix  $\mathbf{H}$ . Difficult to treat directly, the expectation (8) is

evaluated in Appendix A using the replica method in the *large-system limit*, which refers to the regime where the numbers of transmit and receive antennas both go to infinity with their ratio  $K/N$  converging to a positive number  $\alpha$ , called the load of the system. A pair of fixed-point equations are found from which the average transmit energy can be evaluated using the load, the alphabets, as well as the statistics of the data  $s$  and the channel matrix  $\mathbf{H}$ . In particular, the statistics of the channel matrix enter the equations only through the so-called R-transform of the asymptotic distribution of a scalar function of its singular values.

**DEFINITION 1 (R-TRANSFORM)** Let  $P(x)$  denote an arbitrary probability distribution. Let

$$m(s) = \int \frac{dP(x)}{x-s} \quad (9)$$

which is known as the Stieltjes transform. Then, the R-transform of  $P(x)$  is

$$R(w) = m^{-1}(-w) - \frac{1}{w} \quad (10)$$

with  $m^{-1}(\cdot)$  denoting the inverse function of  $m(\cdot)$ .

The following proposition quantifies the average minimum transmit energy using nonlinear precoding.

**PROPOSITION 1** Suppose a random matrix  $\mathbf{J}$  can be decomposed as

$$\mathbf{J} = \mathbf{U}\mathbf{D}\mathbf{U}^\dagger \quad (11)$$

where  $\mathbf{D}$  is diagonal and  $\mathbf{U}$  is Haar distributed [20]. Moreover, as  $K \rightarrow \infty$ , the empirical distribution of the diagonal elements of  $\mathbf{D}$  (i.e., the eigenvalues of  $\mathbf{J}$ ) converges to a non-random distribution uniquely characterized by its R-transform  $R(\cdot)$ . Also, let the empirical distribution of  $s_k$ ,  $k = 1, \dots, K$  converge in probability to some limiting distribution  $P(s)$  as  $K \rightarrow \infty$ . Then under some technical assumptions which are discussed in Appendix A and include, e.g., replica symmetry, the average minimum transmit energy per symbol

$$E = \frac{1}{K} \min_{\mathbf{x} \in \mathcal{B}_{s_1} \times \dots \times \mathcal{B}_{s_K}} \mathbf{x}^\dagger \mathbf{J} \mathbf{x} \rightarrow q [R(-\chi) - \chi R'(-\chi)] \quad (12)$$

in probability as  $K \rightarrow \infty$ . In (12),  $R'(\cdot)$  represents the derivative of the function  $R(\cdot)$ ,  $\chi \in (0, \infty)$  and the parameters  $q$  and  $\chi$  satisfy the following pair of coupled fixed-point equations:

$$q = \sum_{s \in \mathcal{S}} P(s) \int_{\mathbb{C}} \left| \operatorname{argmin}_{x \in \mathcal{B}_s} \left| z - \frac{R(-\chi)x}{\sqrt{qR'(-\chi)}} \right| \right|^2 \frac{e^{-|z|^2}}{\pi} dz \quad (13)$$

$$\chi = \frac{\sum_{s \in \mathcal{S}} P(s) \Re \int_{\mathbb{C}} \operatorname{argmin}_{x \in \mathcal{B}_s} \left| z - \frac{R(-\chi)x}{\sqrt{qR'(-\chi)}} \right| z^* \frac{e^{-|z|^2}}{\pi} dz}{\sqrt{qR'(-\chi)}} \quad (14)$$

where the integrals are carried out for the real and imaginary parts of  $z$  separately from  $-\infty$  to  $\infty$ , and the operator  $\Re$  in (14) takes the real part of the result of the integral.

We remark that even though Proposition 1 describes the minimum energy per symbol in the limit of infinite number of antennas with technical assumptions yet to be fully justified, it is usually a good approximation for systems of moderate size (e.g.  $4 \times 4$  antennas).

From (13) it can be seen that  $q$  describes roughly the extent to which the whole alphabet space is utilized: the larger  $q$  becomes the larger values in  $\mathcal{B}$  are being actively used. This can be also seen by the fact that  $\min_{x \in \mathcal{B}} |x|^2 \leq q \leq \max_{x \in \mathcal{B}} |x|^2$ . The physical intuition behind the energy minimization in the above proposition is the following: In the large system limit the eigenvalue distribution of the matrix  $\mathbf{J}$  becomes deterministic. This distribution is described by the R-transform. When minimizing the transmit energy, the precoder ideally would like to find a vector  $\mathbf{x}$ , which is parallel to the complex eigenvector of the matrix  $\mathbf{J}$  with the minimum eigenvalue and has small norm. However, since the vector  $\mathbf{x}$  is constrained to have elements from the given alphabet  $\mathcal{B}$ , the probability of finding such a vector is zero. Therefore there are two competing options. One is to expand the utilization of the alphabet  $\mathcal{B}$  to higher energy letters, thereby tending to increase the value of  $q$  and accordingly the transmitted energy. The other is to try to find a vector  $\mathbf{x}$  with components increasingly spilling over to eigenvectors with higher eigenvalues, thereby being able to decrease the utilization of high energy letters of  $\mathcal{B}$ , but paying the price of higher eigenvalues of  $\mathbf{J}$ . This eigenvalue spillover loosely determines the value of  $\chi$ . The competition of these two effects is optimized at the minimum, which is determined by the fixed-point equations above. It is clear that the more relaxed the space of the alphabet is, e.g. complex letters versus real ones, the better the precoder will be able to approximate the small eigenvalue eigenvectors.

We note that the proposition applies to every linear front end which can be decomposed according to (11) with Haar distributed eigenspace, which is more general than, e.g. the pseudoinverse described in (2). Such frontends include “regularized” matrices  $\mathbf{H}^\dagger (\mathbf{H}\mathbf{H}^\dagger + \gamma \mathbf{I})^{-1}$  with any  $\gamma > 0$ , which have been studied in [21] in the context of linear precoding.

#### IV. PARTICULAR RESULTS

This section applies the general results presented in Section III to particular wireless MIMO channels and signaling schemes for nonlinear precoding. Proposition 1 leaves three characteristics to specify: 1) the statistics of the channel matrix, which enter the fixed-point equations via its R-transform; 2) the probability mass function  $P(s)$  on the original constellation  $\mathcal{S}$ ; and 3) the relaxed signal alphabets  $\mathcal{B}_s$ ,  $s \in \mathcal{S}$ .

To model the statistics of the entries of the  $K \times N$  matrix  $\mathbf{H}$  is a non-trivial task and a topic of ongoing research (see e.g. [22] and references therein). For the sake of convenience, we assume in this first-order approach that the entries of the channel matrix  $\mathbf{H}$  are independent identically distributed (i.i.d.) circularly-symmetric complex Gaussian random variables with zero mean and variance  $1/N$ . The normalization of each row of  $\mathbf{H}$  to unit norm ensures that the trace of  $\mathbf{H}\mathbf{H}^\dagger$  does not scale with the number of columns in  $\mathbf{T}$  and thus the received energy per symbol without precoding is independent of the

TABLE I  
ENERGY PER SYMBOL FOR INVERTED SQUARE CHANNEL.

$L$	1	2	3	4	$\infty$
$E$	$\infty$	2.6942	2.6656	2.6655	2.6655
$E$ [dB]	$\infty$	4.3043	4.2579	4.2578	4.2578

number of transmit antennas  $N$ .<sup>1</sup> For that case, we find in Appendix B that

$$R(w) = \frac{1 - \alpha - \sqrt{(1 - \alpha)^2 - 4\alpha w}}{2\alpha w} \quad (15)$$

$$R'(w) = \frac{\left(1 - \alpha - \sqrt{(1 - \alpha)^2 - 4\alpha w}\right)^2}{4\alpha w^2 \sqrt{(1 - \alpha)^2 - 4\alpha w}} \quad (16)$$

with  $\alpha = \lim_{K \rightarrow \infty} K/N$ . It is also helpful to recognize that

$$\frac{R^2(w)}{R'(w)} = \frac{\sqrt{(1 - \alpha)^2 - 4\alpha w}}{\alpha}. \quad (17)$$

With the R-transform given in (15), we find by (12)

$$E = \frac{q}{\sqrt{(1 - \alpha)^2 + 4\alpha\chi}} = \frac{q R'(-\chi)}{\alpha R^2(-\chi)}. \quad (18)$$

Plugging that relation into the fixed-point equations in Proposition 1, we obtain the fixed-point equation for the transmit energy per symbol as

$$E = \frac{\sum_{s \in \mathcal{S}} P(s) \int \left| \operatorname{argmin}_{x \in \mathcal{B}_s} \left| z - \frac{x}{\sqrt{\alpha E}} \right| \right|^2 \frac{e^{-|z|^2}}{\pi} dz}{1 - \alpha + \sum_{s \in \mathcal{S}} \frac{2P(s)}{\sqrt{E/\alpha}} \Re \int \operatorname{argmin}_{x \in \mathcal{B}_s} \left| z - \frac{x}{\sqrt{\alpha E}} \right| z^* \frac{e^{-|z|^2}}{\pi} dz}. \quad (19)$$

In the following, we compare the performances of several constructions of the redundant signal re-representations for the channel model specified above.

#### A. One-Dimensional Lattice for Precoding of BPSK Symbols

Consider BPSK modulation with each symbol equally likely to take the two values in  $\mathcal{S} = \{-1, 1\}$ . Let the relaxed alphabets be symmetric:  $\mathcal{B}_1 = -\mathcal{B}_{-1} \subset \mathbb{R}$ . Plugging into (19), the fixed-point equation simplifies to

$$E = \frac{\int \left| \operatorname{argmin}_{x \in \mathcal{B}_1} |z\sqrt{\alpha E} - x| \right|^2 \frac{e^{-|z|^2}}{\pi} dz}{1 - \alpha + 2\sqrt{\frac{\alpha}{E}} \Re \int \operatorname{argmin}_{x \in \mathcal{B}_1} |z\sqrt{\alpha E} - x| z^* \frac{e^{-|z|^2}}{\pi} dz}. \quad (20)$$

Without loss of generality, let  $\mathcal{B}_1 = \{c_1, c_2, \dots, c_L\}$  with  $-\infty = c_0 < c_1 < \dots < c_L < c_{L+1} = +\infty$ . This case describes Tomlinson-Harashima type of precoding [8], [9] with optimization over  $L$  possible representations for each information bit. The boundary points of the Voronoi regions are  $v_i = (c_i + c_{i-1})/2$  and for all  $z \in (v_i/\sqrt{\alpha E_s}, v_{i+1}/\sqrt{\alpha E})$ ,

$$\operatorname{argmin}_{x \in \mathcal{B}_1} |z\sqrt{\alpha E} - x| = c_i. \quad (21)$$

<sup>1</sup>Note that Proposition 1 describes the large-system limit and we do not compare the performance for different  $N$ . Thus the normalization of the channel coefficients does not violate any physical constraint.

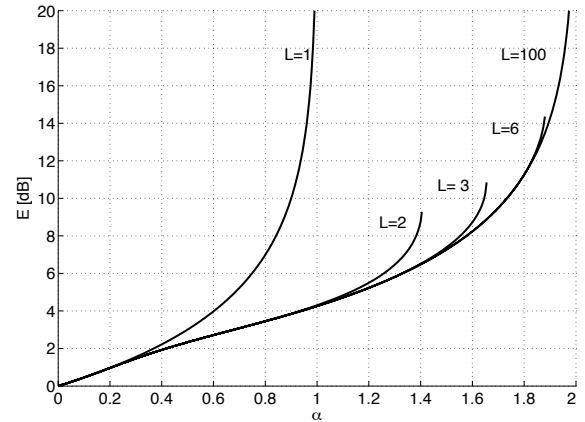


Fig. 1. The transmitted energy per symbol versus the load for various  $L$  corresponding to the one-dimensional lattice precoding for BPSK, using (22) and (23) as discussed in Sec. IV-A.

The fixed-point equation becomes

$$E = \frac{c_1^2 + \sum_{i=2}^L (c_i^2 - c_{i-1}^2) Q\left(\frac{c_i + c_{i-1}}{\sqrt{2\alpha E}}\right)}{1 - \alpha + \sqrt{\alpha} \sum_{i=2}^L \frac{c_i - c_{i-1}}{\sqrt{\pi E}} \exp\left(-\frac{(c_i + c_{i-1})^2}{4\alpha E}\right)} \quad (22)$$

where  $Q(x) = \int_x^\infty \exp(-x^2/2) dx / \sqrt{2\pi}$  denotes the complement of the cumulative distribution function of the standard Gaussian distribution.

For the case of no precoding at all, i.e.  $L = 1$ , we get

$$E = c_1^2 / (1 - \alpha). \quad (23)$$

For the case of general  $L$ , we restrict to the special case of a square channel matrix first. The rectangular channel is addressed subsequently.

1) *Square Channel Matrix*: For  $\alpha = 1$ , (22) simplifies to

$$E = \pi \left[ \frac{c_1^2 + \sum_{i=2}^L (c_i^2 - c_{i-1}^2) Q\left(\frac{c_i + c_{i-1}}{\sqrt{2E}}\right)}{\sum_{i=2}^L (c_i - c_{i-1}) \exp\left(-\frac{(c_i + c_{i-1})^2}{4E}\right)} \right]^2. \quad (24)$$

Numerical solutions to (24) are shown in Table I for the equally spaced integer lattice  $\mathcal{B}_1 = \{+1, -3, +5, -7, +9, \dots\}$  and various numbers of lattice points.

Obviously, there is little improvement when going from two to three lattice points and negligible improvement beyond three. This has significant implications on the potential complexity of a lattice search.

2) *Rectangular Channel Matrix*: For a rectangular channel matrix, the Gramian is only invertible for loads  $\alpha \leq 1$ . However, the R-transform is well-defined for any positive load. For singular random matrices, the R-transform reflects the fact that the asymptotic eigenvalue distribution has some point mass at infinity.

The minimum of the transmit power is determined by (22) and shown in Fig. 1. We observe two distinct behaviors. In the case without precoding, i.e.  $L = 1$ , the energy per symbol goes to infinity in the limit  $\alpha = 1$ . In contrast, the curves

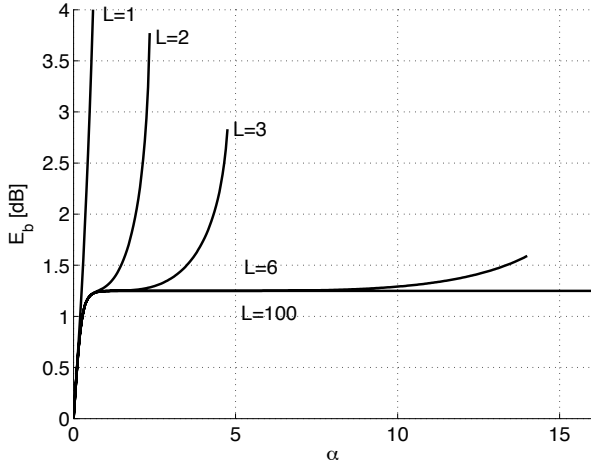


Fig. 2. Transmitted energy per bit (26) versus the load for precoded channel inversion and Gray-mapped QPSK using a two-dimensional quadrature lattice (25), analyzed in Sec. IV-B.

for  $L > 1$  are finite for all  $\alpha \leq 1$ . In fact, a phase transition occurs and the energy per symbol jumps discontinuously from a finite value to infinity at some value of  $\alpha^* > 1$ . Note that precoding enables to achieve finite transmitted energy even for loads  $\alpha \in [1, \alpha^*)$  for which the matrix  $\mathbf{J}$  is singular. This is possible as the degrees of freedom given by the choice of a particular lattice point allow to choose the transmitted vector  $\mathbf{t}$  to lie in a subspace spanned by only those eigenvectors of the matrix  $\mathbf{H}\mathbf{H}^\dagger$  which correspond to non-zero eigenvalues.

### B. Two-Dimensional Quadrature Lattice for QPSK

Consider extending the one-dimensional precoding of BPSK on the real line to two-dimensional precoding of quadrature phase-shift keying (QPSK) in the complex plane. Using Gray mapping, we can consider the precoding for QPSK as independent precoding of BPSK in the real and imaginary components. The original constellation is  $\mathcal{S} = \{1 + j, -1 + j, -1 - j, 1 - j\}$ . The relaxed alphabets are represented as

$$\mathcal{B}_s = \frac{s}{1+j}((4\mathbb{Z} + 1) \times (4j\mathbb{Z} + j)), \quad \forall s \in \mathcal{S}. \quad (25)$$

For example, the relaxed alphabet corresponding to  $1 + j$  is the 2-dimensional lattice  $\mathcal{B}_{1+j} = \{(4\mathbb{Z} + 1) \times (4j\mathbb{Z} + j)\}$ .

The symmetry in both quadrature components implies that (19) becomes

$$E = \frac{c_1^2 + \sum_{i=2}^L (c_i^2 - c_{i-1}^2) Q\left(\frac{c_i + c_{i-1}}{\sqrt{2\alpha E}}\right)}{\frac{1-\alpha}{2} + \sqrt{\alpha} \sum_{i=2}^L \frac{c_i - c_{i-1}}{\sqrt{\pi E}} \exp\left(-\frac{(c_i + c_{i-1})^2}{4\alpha E}\right)}. \quad (26)$$

In order for a fair comparison with one-dimensional modulation, we use the energy per bit  $E_b = E/\log_2 |\mathcal{S}|$  as a metric, where the cardinality of the constellation  $|\mathcal{S}| = 4$  in the case of QPSK. The energy per bit is shown in Fig. 2. Remarkably, the energy per bit remains as small as  $E_b = \frac{4}{3}$  for any load if  $L$  grows large.

### C. 2-Dimensional Checkerboard Lattice for BPSK

One can also relax the one-dimensional BPSK modulation to precoding using lattices in the two-dimensional complex plane. Let  $\mathcal{S} = \{-1, +1\}$ . We may choose

$$\mathcal{B}_s = e^{j\frac{s\pi}{4}}((2\mathbb{Z} + 1) \times (2\mathbb{Z})), \quad s \in \mathcal{S}. \quad (27)$$

The relaxed alphabets  $\mathcal{B}_{+1}$  and  $\mathcal{B}_{-1}$  correspond to the center of the black and white fields of a checkerboard respectively.

We can rotate the above infinite lattice by  $45^\circ$  degrees without loss of generality due to the rotational invariance of the complex Gaussian integral kernel in the fixed-point equation (19). After rotation we find the same lattice as in the two-dimensional quadrature precoding except for a lattice scaling by a factor of  $1/\sqrt{2}$ . Thus, the energy per symbol will be half the energy per symbol of quadrature precoding and the energy per bit will be identical.

### D. Two-Dimensional Semi-Discrete Lattice for BPSK

Consider the following modification of the precoding scheme in Section IV-C. We map each BPSK symbol to a complex number, the real part of which takes its value in the real-valued lattice, whereas the imaginary part is allowed to take any value, which obviously preserves the minimum distance between the relaxed alphabets. Precisely, let  $\mathcal{S}$  and  $\mathcal{B}_s$ ,  $s \in \mathcal{S}$  be defined as in Section IV-A. The new relaxed alphabets will be  $\mathcal{B}_s \times j\mathbb{R}$ ,  $s \in \mathcal{S}$ . By complete relaxation of the imaginary part, we expect the minimum energy to be further reduced. The fixed-point equation (19) reduces to

$$E = \frac{c_1^2 + \sum_{i=2}^L (c_i^2 - c_{i-1}^2) Q\left(\frac{c_i + c_{i-1}}{\sqrt{2\alpha E}}\right)}{1 - \frac{\alpha}{2} + \sqrt{\alpha} \sum_{i=2}^L \frac{c_i - c_{i-1}}{\sqrt{\pi E}} \exp\left[-\frac{(c_i + c_{i-1})^2}{4\alpha E}\right]}. \quad (28)$$

Fig. 3 compares the complex semi-discrete lattice with the complex quadrature lattice in terms of the energy per bit. Precoding with semi-discrete lattices achieves a remarkable gain which comes at the expense of reduced data rate. It is particularly noteworthy that the semi-discrete lattice with  $L = 1$  outperforms all quadrature lattices for loads up to  $\alpha \approx 0.479$ . Note that for  $L = 1$ , the alphabets  $\mathcal{B}_s$  are convex, so that the quadratic programming problem is convex and admits a polynomial time algorithm. For large loads and large lattice size, the energy per bit approaches  $E_b = \frac{4}{3}$ . Oftentimes, using simple convex alphabets not only allows low-complexity implementation of nonlinear precoding, but also leads to good performance.

### E. A Convex Relaxation for QPSK

Consider the following relaxation of the QPSK constellation

$$\mathcal{B}_{1+j} = \{z \in \mathbb{C} : \Re z \geq 1, \Im z \geq 1\} \quad (29)$$

and  $\mathcal{B}_s = \frac{s}{1+j}\mathcal{B}_{1+j}$  for  $s = -1 + j, -1 - j$  and  $1 - j$ , i.e., all alphabets are defined as a rotation of  $\mathcal{B}_{1+j}$  about the origin as depicted in Fig. 4. The mapping  $s \mapsto \mathcal{B}_s$  preserves the minimum distance. As all four alphabets are convex, the corresponding quadratic programming problems can be solved

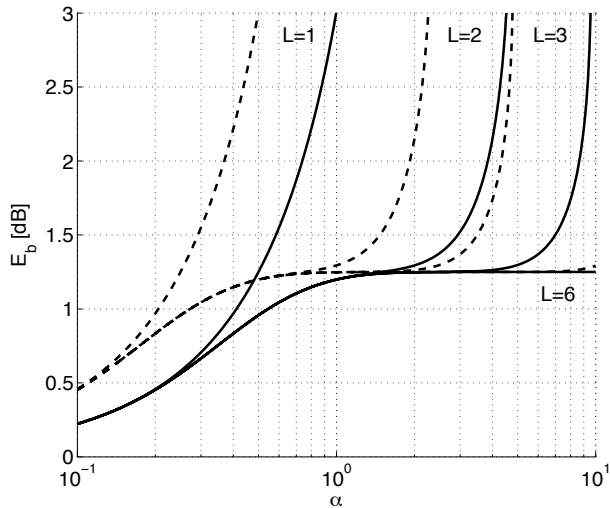


Fig. 3. Comparison between the energy per bit for precoding with the semidiscrete lattice (solid lines) using (28) as discussed in Sec. IV-D with the energy per bit using the complex quadrature lattice (see Fig. 2 and (26) in Sec. IV-B).

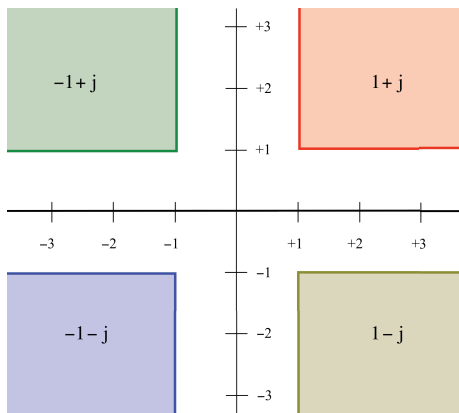


Fig. 4. Convex alphabets corresponding to the QPSK constellation points as discussed in Sec. IV-E.

efficiently. Furthermore, the mappings in the two quadrature components are independent.

Using the above relaxed alphabets, the fixed-point equation (19) simplifies to

$$Q\left(\sqrt{\frac{2}{\alpha E}}\right) = \frac{2 + (\alpha - 1)E + \sqrt{\frac{\alpha E}{\pi}} e^{-\frac{1}{\alpha E}}}{2 + \alpha E}. \quad (30)$$

The solution to (30) is shown in Fig. 5. For unit load, the energy per symbol is found to be approximately three times higher than with lattice precoding. This is the price to pay for precoding with polynomial complexity. In contrast to channel inversion only, the proposed convex relaxation allows to increase the load by about 30% without need for more transmitted energy. Alternatively, the transmitter can achieve the same performance with 30% fewer antennas.

The considerations in the above paragraph concerning the performance of the proposed convex relaxation are somewhat pessimistic. Admittedly, the energy per symbol is about three times larger than with lattice precoding. However, unlike

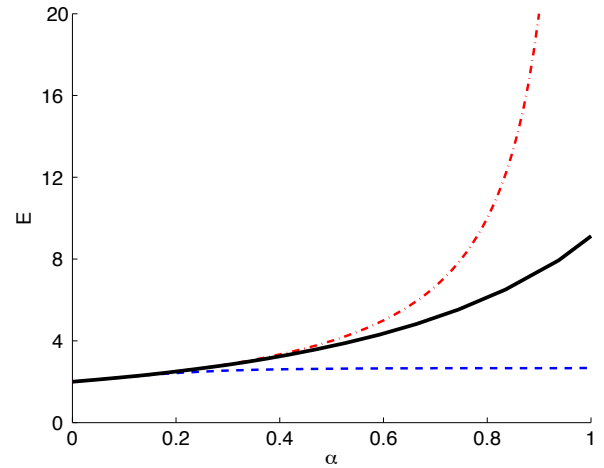


Fig. 5. Energy per symbol versus the load for QPSK. The solid line shows the convex relaxation (see Fig. 4) analyzed in Sec. IV-E. The dashed and dash-dotted lines refer to the complex quadrature lattice with  $L = \infty$  and  $L = 1$ , resp. See (26) and Fig. 2.

lattice precoding, the proposed convex relaxation increases the average distance and, therefore, makes the signal more robust against channel impairments.

## V. CONCLUSIONS

It has been shown quantitatively in this paper that vector precoding can be used to significantly reduce the transmit power in MIMO systems. In particular, we find substantial advantage of complex-valued precoding over real-valued precoding. Moreover, we broaden the scope of nonlinear precoding to include convex alphabets, for which efficient algorithms exist for computing the transmit signal with the minimum energy. We note that the replica symmetry assumption underlying the theoretical result might not hold true. We have started investigating first order replica symmetry breaking (1RSB). Preliminary results indicate that the results in this paper change insignificantly under 1RSB.

## ACKNOWLEDGMENTS

R. Müller and D. Guo would like to thank the Institute for Mathematical Sciences at the National University of Singapore for hosting their visit in 2006, during which this work was initiated. The authors would also like to thank Benjamin Zaidel and Rodrigo de Miguel for carefully proof-reading the final manuscript.

## APPENDIX A

### DERIVATION OF PROPOSITION 1

Let us use  $\mathcal{B}_s$  as a short hand for  $\mathcal{B}_{s_1} \times \dots \times \mathcal{B}_{s_K}$ . We start by rewriting the energy per symbol defined in (12) as

$$E = \lim_{K \rightarrow \infty} \frac{1}{K} \min_{\mathbf{x} \in \mathcal{B}_s} \mathbf{x}^\dagger \mathbf{J} \mathbf{x} \quad (31)$$

$$= - \lim_{K \rightarrow \infty} \lim_{\beta \rightarrow \infty} \frac{1}{\beta K} \mathbb{E} \log \sum_{\mathbf{x} \in \mathcal{B}_s} e^{-\beta \mathbf{x}^\dagger \mathbf{J} \mathbf{x}} \quad (32)$$

where (32) follows from the fact that the infinity norm of a vector gives its maximal component and the introduction of the

expectation results from taking into account the fundamental (postulated) self-averaging property of large random matrices [20]:

ASSUMPTION 1 (SELF-AVERAGING PROPERTY) *We have*

$$\lim_{K \rightarrow \infty} \Pr \left( \frac{1}{K} \left| \min_{\mathbf{x} \in \mathcal{B}_s} \mathbf{x}^\dagger \mathbf{J} \mathbf{x} - \mathbb{E} \min_{\mathbf{x} \in \mathcal{B}_s} \mathbf{x}^\dagger \mathbf{J} \mathbf{x} \right| > \epsilon \right) = 0 \quad (33)$$

for all  $\epsilon > 0$ , i.e. convergence in probability.

We are now faced with a formidable task of calculating the expectation of a logarithm of a sum of exponentials. To make progress we observe that we can rewrite the logarithm as a derivative of a product, namely

$$\mathbb{E} \log Z = \frac{d}{dn} \mathbb{E} Z^n \Big|_{n=0^+} = \frac{d}{dn} \log \mathbb{E} Z^n \Big|_{n=0^+} \quad (34)$$

where the derivatives are evaluated taking the limit  $n = 0$  from the positive real axis, and an extra logarithm is introduced in the second equality for future convenience. One can then rewrite (31) as

$$E = - \lim_{K \rightarrow \infty} \lim_{\beta \rightarrow \infty} \frac{1}{\beta K} \lim_{n \rightarrow 0^+} \frac{\partial}{\partial n} \log \mathbb{E} \left[ \sum_{\mathbf{x} \in \mathcal{B}_s} e^{-\beta \mathbf{x}^\dagger \mathbf{J} \mathbf{x}} \right]^n \quad (35)$$

using (34). We see that by the manipulation described above, we have exchanged the task of calculating an expectation of a logarithm to calculating an expectation of a non-integer power, an equally complicated feat. Nevertheless, we will calculate the above power for integer values of  $n = 1, 2, \dots$  and insist that the analytic continuation of the result in the vicinity of  $n = 0^+$  will be the above function. This is summarized in the following assumption:

ASSUMPTION 2 (REPLICA CONTINUITY) *For all  $\beta > 0$ , the continuation of the function*

$$f(n) = \prod_{a=1}^n \sum_{\mathbf{x}_a \in \mathcal{B}_s} e^{-\beta \mathbf{x}_a^\dagger \mathbf{J} \mathbf{x}_a} \quad (36)$$

onto the positive real line is equal to

$$\left( \sum_{\mathbf{x} \in \mathcal{B}_s} e^{-\beta \mathbf{x}^\dagger \mathbf{J} \mathbf{x}} \right)^n \quad (37)$$

in the right-sided vicinity of  $n = 0$ .

This is the basis of the so-called replica approach: Rather than trying to evaluating an expectation over the logarithm of a function, we opt to calculate the expectation of the product of  $n$  identical replicas of that function and then analytically continue the result to real-valued  $n$  in the vicinity of zero. This trick has been used extensively, with little formal justification but with many celebrated results in statistical physics [23]. Applying this trick, and after interchanging the limits of  $K \rightarrow \infty$  and  $n \rightarrow 0$  we have

$$E = - \lim_{\beta \rightarrow \infty} \frac{1}{\beta} \lim_{n \rightarrow 0} \frac{\partial}{\partial n} \Xi_n \quad (38)$$

where<sup>2</sup>

$$\Xi_n = \lim_{K \rightarrow \infty} \frac{1}{K} \log \mathbb{E} \prod_{a=1}^n \sum_{\mathbf{x}_a \in \mathcal{B}_s} e^{-\beta \mathbf{x}_a^\dagger \mathbf{J} \mathbf{x}_a} \quad (39)$$

$$= \lim_{K \rightarrow \infty} \frac{1}{K} \log \mathbb{E} \sum_{\{\mathbf{x}_a \in \mathcal{B}_s\}} \exp \left[ -\beta \sum_{a=1}^n \mathbf{x}_a^\dagger \mathbf{J} \mathbf{x}_a \right] \quad (40)$$

$$= \lim_{K \rightarrow \infty} \frac{1}{K} \log \mathbb{E} \sum_{\{\mathbf{x}_a \in \mathcal{B}_s\}} \exp \left[ \text{tr} \left( -\beta \mathbf{J} \sum_{a=1}^n \mathbf{x}_a \mathbf{x}_a^\dagger \right) \right] \quad (41)$$

It is important to keep in mind that we will need the *linear* term in a small  $n$  expansion of  $\Xi_n$ , in order to evaluate the derivative in (38) at  $n = 0$ . Expressing now,  $\mathbf{J} = \mathbf{U} \mathbf{D} \mathbf{U}^\dagger$ , as in (11), we can integrate over the Haar distributed eigenvectors of  $\mathbf{J}$ . This integration was studied by Harish-Chandra [24] and Itzykson & Zuber [25] in the mathematics and physics literature, respectively. It was recently re-derived in the context of wireless communications in [26]. Here, we are interested in the asymptotic form of the Harish-Chandra-Itzykson-Zuber integral, evaluated for fixed-rank matrices  $\sum_a \mathbf{x}_a \mathbf{x}_a^\dagger$ , when  $K \rightarrow \infty$ . This result was applied in the context of wireless communications in [27]. Guionnet and Maïda [28] solve this integral in terms of the R-transform  $R(w)$  of the asymptotic eigenvalue distribution of  $\mathbf{J}$ . Following their approach yields

$$\Xi_n = \lim_{K \rightarrow \infty} \frac{1}{K} \log \sum_{\{\mathbf{x}_a \in \mathcal{B}_s\}} \exp \left[ -K \sum_{a=1}^n \int_0^{\lambda_a} R(-w) dw \right] \quad (42)$$

with  $\lambda_1, \dots, \lambda_n$  denoting the eigenvalues of the  $n \times n$  dimensional matrix  $\beta \mathbf{Q}$ , where  $\mathbf{Q}$  is defined by

$$Q_{ab} = \frac{1}{K} \mathbf{x}_a^\dagger \mathbf{x}_b \triangleq \frac{1}{K} \sum_{k=1}^K x_{ak}^* x_{bk} \quad (43)$$

In order to perform the summation in (42), the  $Kn$ -dimensional space spanned by the replicas is split into subshells

$$S(\mathbf{Q}) \triangleq \{ \mathbf{x}_1, \dots, \mathbf{x}_n \mid \mathbf{x}_a^\dagger \mathbf{x}_b = K Q_{ab} \} \quad (44)$$

where the inner product of two replicated vectors  $\mathbf{x}_a$  and  $\mathbf{x}_b$  is constant in each subshell. Noting that  $\mathbf{x}_a^\dagger \mathbf{x}_b$  is Hermitian, we can express  $\Xi_n$  as

$$\Xi_n = \lim_{K \rightarrow \infty} \frac{1}{K} \log \int e^{K\mathcal{I}(\mathbf{Q})} e^{-K\mathcal{G}(\mathbf{Q})} \mathcal{D}\mathbf{Q}, \quad (45)$$

where

$$\mathcal{D}\mathbf{Q} = \prod_{a=1}^n dQ_{aa} \prod_{b=a+1}^n d\Re Q_{ab} d\Im Q_{ab} \quad (46)$$

is the appropriate integration measure (note that  $\mathbf{Q}^\dagger = \mathbf{Q}$ ),

$$\mathcal{G}(\mathbf{Q}) = \sum_{a=1}^n \int_0^{\lambda_a(\beta \mathbf{Q})} R(-w) dw \quad (47)$$

and

$$e^{K\mathcal{I}(\mathbf{Q})} = \sum_{\{\mathbf{x}_a \in \mathcal{B}_s\}} \prod_{a=1}^n \delta(\mathbf{x}_a^\dagger \mathbf{x}_a - K Q_{aa}) \times \prod_{b=a+1}^n \delta(\Re[\mathbf{x}_a^\dagger \mathbf{x}_b - K Q_{ab}]) \delta(\Im[\mathbf{x}_a^\dagger \mathbf{x}_b - K Q_{ab}]) \quad (48)$$

<sup>2</sup>The notation  $\sum_{\{\mathbf{x}_a \in \mathcal{B}_s\}}$  is used as shortcut for  $\sum_{\mathbf{x}_1 \in \mathcal{B}_s} \dots \sum_{\mathbf{x}_n \in \mathcal{B}_s}$ .

denotes the probability weight of the subshell. There are two reasons of following this procedure and introducing the new variables  $Q_{ab}$ . First, this allows us to explicitly sum over  $\{\mathbf{x}_a\}$  as will be seen below. Secondly, we expect that for large  $K$  a single subshell will dominate  $\Xi_n$ , which will also be observed below. In the following the two exponential terms in (45) are evaluated separately.

We start with the evaluation of the measure  $e^{KT(\mathbf{Q})}$ . For future convenience, we introduce the complex variables  $\tilde{Q}_{ab}^{(I)}, 1 \leq a \leq b \leq n$  and  $\tilde{Q}_{ab}^{(Q)}, 1 \leq a < b \leq n$ . We also define the matrix  $\tilde{\mathbf{Q}}$  with elements

$$\tilde{Q}_{aa} = \tilde{Q}_{aa}^{(I)} \quad (49)$$

$$\tilde{Q}_{ab} = \frac{1}{2} \left( \tilde{Q}_{ab}^{(I)} - j\tilde{Q}_{ab}^{(Q)} \right) \quad (50)$$

$$\tilde{Q}_{ba} = \frac{1}{2} \left( \tilde{Q}_{ab}^{(I)} + j\tilde{Q}_{ab}^{(Q)} \right) \quad (51)$$

where  $a < b$ . We may now write the Dirac measure of the elements of the Hermitian matrix  $P_{ab} = \mathbf{x}_a^\dagger \mathbf{x}_b - KQ_{ab}$  in terms of its inverse Laplace transform

$$\delta(P_{aa}) = \int_{\mathcal{J}} \exp \left[ \tilde{Q}_{aa} P_{aa} \right] \frac{d\tilde{Q}_{aa}^{(I)}}{2\pi j} \quad (52)$$

$$\delta(\Re P_{ab}) \delta(\Im P_{ab}) = \int_{\mathcal{J}^2} e^{\tilde{Q}_{ab}^{(I)} \Re P_{ab} - \tilde{Q}_{ab}^{(Q)} \Im P_{ab}} \frac{d\tilde{Q}_{ab}^{(I)} d\tilde{Q}_{ab}^{(Q)}}{(2\pi j)^2} \quad (53)$$

$$= \int_{\mathcal{J}^2} e^{\tilde{Q}_{ab} P_{ba} + \tilde{Q}_{ba} P_{ab}} \frac{d\tilde{Q}_{ab}^{(I)} d\tilde{Q}_{ab}^{(Q)}}{(2\pi j)^2}. \quad (54)$$

with  $\mathcal{J} = (t - j\infty; t + j\infty)$  for some  $t \in \mathbb{R}$  and  $P_{ab} = P_{ba}^*$ . We may now express (48) as

$$e^{KT(\mathbf{Q})} = \sum_{\{\mathbf{x}_a \in \mathcal{B}_s\}} \int_{\mathcal{J}^{n^2}} e^{\sum_{a,b} \tilde{Q}_{ab} (\mathbf{x}_a^\dagger \mathbf{x}_b - KQ_{ab})} \tilde{\mathcal{D}}\tilde{\mathbf{Q}} \quad (55)$$

$$= \int_{\mathcal{J}^{n^2}} e^{-K \text{tr}[\tilde{\mathbf{Q}}\mathbf{Q}] + \sum_{k=1}^K \log M_k(\tilde{\mathbf{Q}})} \tilde{\mathcal{D}}\tilde{\mathbf{Q}} \quad (56)$$

where the integration measure is given by

$$\tilde{\mathcal{D}}\tilde{\mathbf{Q}} = \prod_{a=1}^n \left( \frac{d\tilde{Q}_{aa}^{(I)}}{2\pi j} \prod_{b=a+1}^n \frac{d\tilde{Q}_{ab}^{(I)} d\tilde{Q}_{ab}^{(Q)}}{(2\pi j)^2} \right) \quad (57)$$

and

$$M_k(\tilde{\mathbf{Q}}) = \sum_{\{\mathbf{x}_a \in \mathcal{B}_{s_k}\}} e^{\sum_{a,b} \mathbf{x}_a^\dagger \mathbf{x}_b \tilde{Q}_{ab}}. \quad (58)$$

In the limit of  $K \rightarrow \infty$  one of the exponential terms in (45) will dominate over all others. Thus, only that extremal value of the correlation  $Q_{ab}$  is relevant for calculation of the integral.

To make further progress, we need to identify the saddle-point which dominates the integrals. We invoke an important assumption on the structure of the matrices  $(Q_{ab})$  and  $(\tilde{Q}_{ab})$  at the saddle-point:

**ASSUMPTION 3 (REPLICA SYMMETRY)** *When applying the replica method to solve the saddle-point equations, we will assume that the extremal point is invariant to permutations of the replica indexes.*

The assumption of replica symmetry translates to searching over a subset of possible saddle-points with specific symmetry properties of the matrix  $\mathbf{Q} = (Q_{ab})$ . Indeed, we require that  $Q_{ab} = q, \forall a \neq b$  and  $Q_{aa} = q + \chi/\beta, \forall a$  for some  $q$  and  $\chi$  with  $\chi \geq 0$  since  $\mathbf{Q}$  has to be positive semidefinite. Thus we distinguish the correlation between different replicas and autocorrelation of an individual replica. We apply the same idea to the correlation variables in the transform domain and set with a modest amount of foresight  $\tilde{Q}_{ab} = \beta^2 f^2, \forall a \neq b$  and  $\tilde{Q}_{aa} = \beta^2 f^2 - \beta e, \forall a$ . Note that despite the fact that  $\mathbf{Q}$  is complex-valued in general, its values at the saddle-point are in fact real-valued.

For a detailed discussion of replica symmetry, the reader is referred to the literature of spin glasses, e.g. [12], [29]. Even though naively there is no *a priori* reason for replica symmetry not to hold (after all we start with a bona fide replica symmetric problem (35)), it should be pointed out that, at least for the non-convex problems discussed in this paper, replica symmetry is not generally valid. However, it is well-known in statistical mechanics that the true value of quantities such as  $E$  does not differ much from the corresponding values evaluated within the replica-symmetric assumption (cf. [30], [31]).

For the evaluation of  $\mathcal{G}(\mathbf{Q})$  in (45), we can use replica symmetry to explicitly calculate the eigenvalues  $\lambda_i$ . Considerations of linear algebra lead to the conclusion that the eigenvalues  $\chi$  and  $\chi + \beta n q$  occur with multiplicities  $n-1$  and  $1$ , respectively. Thus we get

$$\mathcal{G}(q, \chi) = (n-1) \int_0^\chi R(-w) dw + \int_0^{\chi + \beta n q} R(-w) dw. \quad (59)$$

Since the integral in (45) is dominated by the maximum argument of the exponential function, the derivatives of

$$\mathcal{G}(q, \chi) + \text{tr}(\tilde{\mathbf{Q}}\mathbf{Q}) \quad (60)$$

with respect to  $q$  and  $\chi$  must vanish as  $K \rightarrow \infty$ .<sup>3</sup> The assumption of replica symmetry leads to

$$\text{tr}(\tilde{\mathbf{Q}}\mathbf{Q}) = n(n-1)\beta^2 f^2 q + n(\beta f^2 - e)(\beta q + \chi). \quad (61)$$

Taking derivatives after plugging (59) and (61) into (60) yields

$$nR(-\chi - \beta n q) + n(n-1)\beta f^2 + n(\beta f^2 - e) = 0 \quad (62)$$

$$(n-1)R(-\chi) + R(-\chi - \beta n q) + n(\beta f^2 - e) = 0 \quad (63)$$

and solving for  $e$  and  $f$  gives

$$e = R(-\chi) \quad (64)$$

$$f = \sqrt{\frac{R(-\chi) - R(-\chi - \beta n q)}{\beta n}} \xrightarrow{n \rightarrow \infty} \sqrt{q R'(-\chi)}. \quad (65)$$

<sup>3</sup>It turns out that when  $\lim_{n \rightarrow 0} \partial_n \Xi_n$  is expressed in terms of  $e, f, q, \chi$ , the relevant extremum is in fact a maximum and not a minimum. This is due to the fact that when  $n$  drops below unity, the minima of a function become maxima and vice-versa. For a detailed analysis of this technicality, see [32].

$$\chi = \frac{1}{\sqrt{qR'(-\chi)}} \iint \frac{\sum_{x \in \mathcal{B}_s} \Re\{z^*x\} e^{\beta 2\sqrt{qR'(-\chi)}\Re\{z^*x\} - \beta R(-\chi)|x|^2}}{\sum_{x \in \mathcal{B}_s} e^{\beta 2\sqrt{qR'(-\chi)}\Re\{z^*x\} - \beta R(-\chi)|x|^2}} Dz dP_s(s) \quad (74)$$

$$q = \iint \frac{\sum_{x \in \mathcal{B}_s} |x|^2 e^{\beta 2\sqrt{qR'(-\chi)}\Re\{z^*x\} - \beta R(-\chi)|x|^2}}{\sum_{x \in \mathcal{B}_s} e^{\beta 2\sqrt{qR'(-\chi)}\Re\{z^*x\} - \beta R(-\chi)|x|^2}} Dz dP_s(s) - \frac{\chi}{\beta}. \quad (75)$$

In addition, the replica symmetry assumption simplifies (58)

$$M_k(e, f) = \sum_{\{x_a \in \mathcal{B}_{s_k}\}} e^{\beta \sum_{a=1}^n [(\beta f^2 - e)|x_a|^2 + 2 \sum_{b=a+1}^n \beta f^2 \Re\{x_a^* x_b\}]} \quad (66)$$

Note that the sets  $\mathcal{B}_{s_k}$  enter the transmitted energy only via (66). Applying the complex Hubbard-Stratonovich transform

$$e^{|x|^2} = \int_{\mathbb{C}} e^{2\Re\{xz^*\}} e^{-|z|^2} \frac{Dz}{\pi} \quad (67)$$

to (66), we find

$$M_k(e, f) = \sum_{\{x_a \in \mathcal{B}_{s_k}\}} e^{\beta^2 f^2 \left| \sum_{a=1}^n x_a \right|^2 - \sum_{a=1}^n \beta e |x_a|^2} \quad (68)$$

$$= \sum_{\{x_a \in \mathcal{B}_{s_k}\}} \int e^{\beta \sum_{a=1}^n 2f \Re\{x_a z^*\} - e |x_a|^2} Dz \quad (69)$$

$$= \int \left( \sum_{x \in \mathcal{B}_{s_k}} e^{2\beta f \Re\{xz^*\} - \beta e |x|^2} \right)^n Dz. \quad (70)$$

Moreover, for  $K \rightarrow \infty$ , we have by the law of large numbers

$$\log M(e, f) = \frac{1}{K} \sum_{k=1}^K \log M_k(e, f) \quad (71)$$

$$\rightarrow \int \log \int \left( \sum_{x \in \mathcal{B}_s} e^{2\beta f \Re\{z^*x\} - \beta e |x|^2} \right)^n Dz dP(s). \quad (72)$$

In the large-system limit, the integral in (56) is dominated by that value of the integration variable which maximizes the exponent. Thus, partial derivatives of

$$\log M(e, f) - \text{tr}(\tilde{Q}Q) \quad (73)$$

with respect to  $f$  and  $e$  must vanish as  $K \rightarrow \infty$ . An explicit calculation of the two derivatives gives the following expressions for the macroscopic parameters  $q$  and  $\chi$  shown on top the page. Finally, the fixed-point equations (74) and (75) simplify via the saddle point integration rule to (14) and (13) in the limit  $\beta \rightarrow \infty$ . Note that the minimization with respect to the symbol  $x$  splits the integration space of  $z$  into the Voronoi regions defined by the (appropriately scaled) signal constellation  $\mathcal{B}_s$ .

Returning to the initial goal of the average transmit energy, and collecting previous results, we find from (38) that

$$\begin{aligned} E &= \lim_{\beta \rightarrow \infty} \frac{1}{\beta} \lim_{n \rightarrow 0} \frac{\partial}{\partial n} \left[ (n-1) \int_0^\chi R(-w) dw \right. \\ &\quad \left. + \int_0^{\chi + \beta n q} R(-w) dw - \log M(e, f) \right. \\ &\quad \left. + n(n-1)f^2\beta^2 q + n(f^2\beta - e)(\chi + \beta q) \right] \quad (76) \\ &= \lim_{\beta \rightarrow \infty} \frac{1}{\beta} \int_0^\chi R(-w) dw - \frac{\chi}{\beta} R(-\chi) + q\chi R'(-\chi) \\ &\quad - \frac{1}{\beta} \iint \log \sum_{x \in \mathcal{B}_s} e^{\beta 2f \Re\{z^*x\} - \beta e |x|^2} Dz dP(s). \quad (77) \end{aligned}$$

We use l'Hospital's rule, re-substitute  $\chi$  and  $q$ , make use of  $0 < \chi < \infty$  and finally obtain (12). Note that for any bound on the amplitude of the signal set  $\mathcal{B}$ , the parameter  $q$  is finite. Even without bound,  $q$  will remain finite for a well-defined minimization problem. The parameter  $\chi$  behaves in a more complicated manner. It can be both zero, finite, and infinite as  $\beta \rightarrow \infty$  depending on the particular R-transform and the signal sets  $\mathcal{B}_s$ . For  $\chi \notin (0, \infty)$ , the saddle-point limits have to be reconsidered.

## APPENDIX B THE R-TRANSFORM

Let  $P_X(x)$  be an arbitrary probability distribution function such that both the Stieltjes transform defined in (9) and

$$m_{X^{-1}}(s) = \int \frac{dP_X(x)}{\frac{1}{x} - s} \quad (78)$$

exist for some complex  $s$  with  $\Im(s) > 0$ . It can be checked that

$$m_{X^{-1}}\left(\frac{1}{s}\right) = -s(1 + s m_X(s)). \quad (79)$$

Let  $s = m_X^{-1}(-w)$ . Then, we find

$$m_{X^{-1}}\left(\frac{1}{m_X^{-1}(-w)}\right) = -m_X^{-1}(-w)(1 - w m_X^{-1}(-w)). \quad (80)$$

and

$$\frac{1}{m_X^{-1}(-w)} = m_X^{-1}(-w)(1 - w m_X^{-1}(-w)). \quad (81)$$

With Definition 1, we find

$$\frac{1}{R_X(w) + \frac{1}{w}} = R_{X^{-1}} \left( -wR_X(w) \left( R_X(w) + \frac{1}{w} \right) \right) - \frac{1}{wR_X(w) \left( R_X(w) + \frac{1}{w} \right)} \quad (82)$$

and

$$\frac{1}{R_X(w)} = R_{X^{-1}} \left( -R_X(w) (1 + wR_X(w)) \right). \quad (83)$$

It is well known [33], [34] that for a  $K \times N$  random matrix  $\mathbf{H}$  with i.i.d. entries of variance  $1/N$ , the R-transform of the limiting spectral measure  $P_{\mathbf{H}\mathbf{H}^\dagger}(x)$  is given by

$$R_{\mathbf{H}\mathbf{H}^\dagger}(w) = \frac{1}{1 - \alpha w}. \quad (84)$$

Letting  $X^{-1} = \mathbf{H}\mathbf{H}^\dagger$ , we find

$$R_{(\mathbf{H}\mathbf{H}^\dagger)^{-1}}(w) = 1 + \alpha R_{(\mathbf{H}\mathbf{H}^\dagger)^{-1}}(w) (1 + wR_{(\mathbf{H}\mathbf{H}^\dagger)^{-1}}(w)) \quad (85)$$

with (83). Solving (85) for the R-transform implies (15). Note that for  $\alpha \geq 1$ , the mean of the spectral measure is diverging. Thus, the R-transform must have a pole at  $w = 0$  which excludes the other solution of (85).

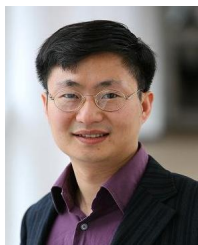
## REFERENCES

- [1] G. Foschini and M. Gans, "On limits of wireless communications in a fading environment when using multiple antennas," *Wireless Personal Communications*, vol. 6, pp. 311–335, 1998.
- [2] I. E. Telatar, "Capacity of multi-antenna Gaussian channels," *European Transactions on Telecommunications*, vol. 10, pp. 585–595, Nov./Dec. 1999.
- [3] B. R. Vojčić and W. M. Jang, "Tranmitter precoding in synchronous multiuser communications," *IEEE Trans. Commun.*, vol. 46, pp. 1346–1355, Oct. 1998.
- [4] M. Joham, W. Utschick, and J. A. Nossek, "Linear transmit processing in MIMO communication systems," *IEEE Trans. Signal Processing*, vol. 53, pp. 2700–2712, Aug. 2005.
- [5] R. F. Fischer, *Precoding and Signal Shaping for Digital Transmission*. John Wiley & Sons, 2002.
- [6] C. Windpassinger, R. F. H. Fischer, T. Vencel, and J. B. Huber, "Precoding in multiantenna and multiuser communications," *IEEE Trans. Wireless Commun.*, vol. 3, pp. 1305–1316, July 2004.
- [7] B. M. Hochwald, C. Peel, and A. Swindlehurst, "A vector-perturbation technique for near-capacity multiantenna multiuser communication-Part II: Perturbation," *IEEE Trans. Commun.*, vol. 53, pp. 537–544, Mar. 2005.
- [8] M. Tomlinson, "New automatic equaliser employing modulo arithmetic," *IEE Electronics Letters*, vol. 7, pp. 138–139, Mar. 1971.
- [9] H. Harashima and H. Miyakawa, "Matched-transmission technique for channels with intersymbol interference," *IEEE Trans. Commun.*, vol. COM-20, pp. 774–780, Aug. 1972.
- [10] S. P. Boyd and L. Vandenberghe, *Convex Optimization*. Cambridge University Press, 2004.
- [11] S. F. Edwards and P. W. Anderson, "Theory of spin glasses," *J. Physics F: Metal Physics*, vol. 5, pp. 965–974, 1975.
- [12] M. Mezard, G. Parisi, and M. A. Virasoro, *Spin Glass Theory and Beyond*. Singapore: World Scientific, 1987.
- [13] T. Tanaka, "A statistical mechanics approach to large-system analysis of CDMA multiuser detectors," *IEEE Trans. Inform. Theory*, vol. 48, pp. 2888–2910, Nov. 2002.
- [14] A. L. Moustakas, S. H. Simon, and A. M. Sengupta, "MIMO capacity through correlated channels in the presence of correlated interferers and noise: A (not so) large N analysis," *IEEE Trans. Inform. Theory*, vol. 49, Oct. 2003.
- [15] R. R. Müller and W. H. Gerstacker, "On the capacity loss due to separation of detection and decoding," *IEEE Trans. Information Theory*, vol. 50, pp. 1769–1778, Aug. 2004.
- [16] D. Guo and S. Verdú, "Randomly spread CDMA: Asymptotics via statistical physics," *IEEE Trans. Information Theory*, vol. 51, pp. 1983–2010, June 2005.
- [17] Y. Kabashima and D. Saad, "Statistical mechanics of error-correcting codes," *Europhysics Letters*, vol. 45, 1999.
- [18] A. Montanari and N. Sourlas, "The statistical mechanics of turbo codes," *The European Physics Journal B*, vol. 18, 2000.
- [19] G. H. Golub and C. F. van Loan, *Matrix Computations*. Baltimore: The Johns Hopkins University Press, 3rd ed., 1996.
- [20] M. L. Mehta, *Random Matrices*. Boston, MA: Academic Press, 2nd ed., 1991.
- [21] C. B. Peel, B. M. Hochwald, and A. L. Swindlehurst, "A vector-perturbation technique for near-capacity multiantenna multiuser communication-Part I: Channel inversion and regularization," *IEEE Trans. Commun.*, vol. 53, pp. 195–202, Jan. 2005.
- [22] M. Debbah and R. Müller, "MIMO channel modelling and the principle of maximum entropy," *IEEE Trans. Inform. Theory*, vol. 51, pp. 1667–1690, May 2005.
- [23] H. Nishimori, *Statistical Physics of Spin Glasses and Information Processing*. Oxford, U.K.: Oxford University Press, 2001.
- [24] Harish-Chandra, "Fourier transforms on a semisimple Lie algebra I," *American J. Mathematics*, vol. 79, pp. 193–257, 1957.
- [25] C. Itzykson and J. Zuber, "The planar approximation (II)," *J. Mathematical Physics*, vol. 21, pp. 411–421, Mar. 1980.
- [26] B. Hassibi and T. L. Marzetta, "Multiple-antennas and isotropically random unitary inputs: The received signal density in closed form," *IEEE Trans. Inform. Theory*, vol. 48, pp. 1473–1484, June 2002.
- [27] K. Takeda, S. Uda, and Y. Kabashima, "Analysis of CDMA systems that are characterized by eigenvalue spectrum," *Europhysics Letters*, vol. 76, no. 6, pp. 1193–1199, 2006.
- [28] A. Guionnet and M. Maïda, "A Fourier view on the R-transform and related asymptotics of spherical integrals," *J. Functional Analysis*, vol. 222, pp. 435–490, 2005.
- [29] K. Fischer and J. Hertz, *Spin Glasses*. Cambridge, U.K.: Cambridge University Press, 1991.
- [30] S. Kirkpatrick and D. Sherrington, "Infinite-ranged models of spin-glasses," *Physics Review B*, vol. 17, no. 11, 1978.
- [31] E. Marinari, G. Parisi, and F. Ritort, "Replica field theory for deterministic models (II): A non-random spin glass with glassy behavior," *J. Physics A: Mathematical and General*, vol. 27, pp. 7647–7668, 1994.
- [32] G. Parisi, "A sequence of approximated solutions to the S-K model for spin glasses," *J. Physics A: Mathematical and General*, vol. 13, 1980.
- [33] D. V. Voiculescu, K. J. Dykema, and A. Nica, *Free Random Variables*. Providence, RI: American Mathematical Society, 1992.
- [34] A. M. Tulino and S. Verdú, "Random matrix theory and wireless communications," *Foundations and Trends in Communications and Information Theory*, vol. 1, June 2004.



**Ralf Müller** (S'96-M'03-SM'05) was born in Schwabach, Germany, 1970. He received the Dipl.-Ing. and Dr.-Ing. degree with distinction from University of Erlangen-Nuremberg in 1996 and 1999, respectively. From 2000 to 2004, he was with Forschungszentrum Telekommunikation Wien (ftw.) in Vienna, Austria and teaching at Vienna University of Technology. Since 2005 he has been a full professor at the Department of Electronics and Telecommunications at the Norwegian University of Science and Technology (NTNU) in Trondheim, Norway. He

held visiting appointments at Princeton University, U.S.A., Institut Eurécom, France, the University of Melbourne, Australia, Oulu University, Finland, the National University of Singapore, Babeş-Bolyai University, Cluj-Napoca, Romania, and Kyoto University, Japan. Dr. Müller received the Leonard G. Abraham Prize (jointly with Sergio Verdú) from the IEEE Communications Society. He was presented awards for his dissertation by the Mannesmann (now Vodafone) Foundation for Mobile Communications and the German Information Technology Society (ITG). He also received the ITG award as well as the Philipp-Reis Prize (jointly with R. Fischer). Dr. Müller served as an associate editor for the IEEE Transactions on Information Theory from 2003 to 2006.



**Dongning Guo** has been an Assistant Professor in the Department of Electrical Engineering & Computer Science at Northwestern University since 2004. He received the Ph.D. and M.Sc. degrees from Princeton University, the M.Eng. degree from the National University of Singapore and the B.Eng. degree from University of Science & Technology of China. He was an R&D Engineer in the Centre for Wireless Communications (now the Institute for Infocom Research), Singapore from 1998 to 1999.

He was a Visiting Professor at Norwegian University of Science and Technology in summer 2006. He received the Huber and Suhner Best Student Paper Award in the International Zurich Seminar on Broadband Communications in 2000 and the National Science Foundation Faculty Early Career Development (CAREER) Award in 2007. His research interests are in information theory, communications and networking.



**Aris Moustakas** (SM'04) received a B.S. degree in physics from Caltech in 1990 and M.S. and Ph.D. degrees in theoretical condensed matter physics from Harvard University in 1992 and 1996, respectively. In 1998, he joined Bell Labs, Lucent Technologies, NJ, first in the Physical Sciences Division and then also in the Wireless Advanced Technology Laboratory. Since 2005 he is an assistant professor at the Physics Dept. of the National Capodistrian University of Athens. His current research interests

lie in the areas of multiple antenna systems, signal processing for smart antennas and the applications of statistical physics methods to the theory of communications and networks.